

Implanting CNT Forest onto Carbon Nanosheets as Multifunctional Hosts for High-Performance Lithium Metal Batteries

Changtai Zhao, Zhao Wang, Xinyi Tan, Huawei Huang, Zhongxin Song, Yipeng Sun, Song Cui, Qianbing Wei, Wei Guo, Ruying Li, Chang Yu,* Jieshan Qiu,* and Xueliang Sun*

Lithium (Li) metal anodes are considered an ideal anode for the next-generation Li batteries with high energy density. However, some intrinsic problems, such as Li dendrite growth and tremendous volume change, inhibit their practical applications. Here, an unstacked microstructure is tailored by planting an N-doped carbon nanotube (CNT) forest on the surface of biomass-derived large-aspect-ratio N-doped carbon sheets (CSs) (CS-CNT), which can effectively overcome the easy aggregation properties of CSs. As the host material for Li metal anode, the N-doping and unstacked natures of CS-CNT offer sufficient Li nucleation sites, large surface area, and space for smooth and uniform Li deposition, effectively preventing the formation of dendritic Li. As a result, the cell with this electrode can keep high and stable Coulombic efficiency of 98.8% for over 2000 h, superior to the pure CSs and Cu foil electrodes. Additionally, the symmetric cell exhibits significantly enhanced cycle life up to 1500 h as well as lowered hysteresis. The present study sheds light on the design of unstacked porous carbon materials and offers an opportunity to develop high efficiency Li metal anode.

1. Introduction

Electrochemical energy storage is one of the key technologies for the efficient utilization of sustainable energy resources and the clean mobile energy supply.^[1] Among various candidates, lithium (Li) metal batteries (LMBs), such as Li–O₂ batteries and Li–S batteries, have drawn ever-increasing attention because of their high theoretical energy densities which originate from the high specific capacities of Li metal and active materials in cathode (O₂ and sulfur) and the lowest reduction potential of Li metal.^[2] However, the formation of dendritic Li in anode and the noneffective cathode are still big challenges in developing LMBs, especially Li–O₂ batteries.^[3] The formation of Li dendrites will decrease the Coulombic efficiency due to the continuous side reactions between Li metal and liquid electrolyte. Moreover, large Li dendrites can penetrate the separator and

reach the cathode, causing short circuits of battery and safety hazards.^[4] Besides, the tremendous volume change during the discharge/charge process is another fatal problem to prohibit the practical application of LMBs based on the thickness change of about 5 μm for 1 mAh cm⁻² of Li metal.^[5] These problems are continuously of concern and urgently need to be overcome.

Considerable efforts have been devoted to exploring effective approaches to addressing issues associated with Li dendrites mentioned above.^[6] For instance, replacing organic liquid electrolytes with solid-state electrolytes that can repress Li dendrites is a strategy to avoid short circuit and enhance safety.^[7] The reinforcement of the solid electrolyte interphase (SEI), which is formed at the interface between the Li metal and the electrolyte, is also a common strategy to protect Li metal by approaches of developing novel electrolytes, modifying the electrolyte with various additives and designing artificial SEI layers.^[8] Moreover, the use of 3D conductive matrix as the host material for Li metal can decrease the local current density and Li ions flux, thus avoiding the formation of Li dendrites.^[9] More importantly,

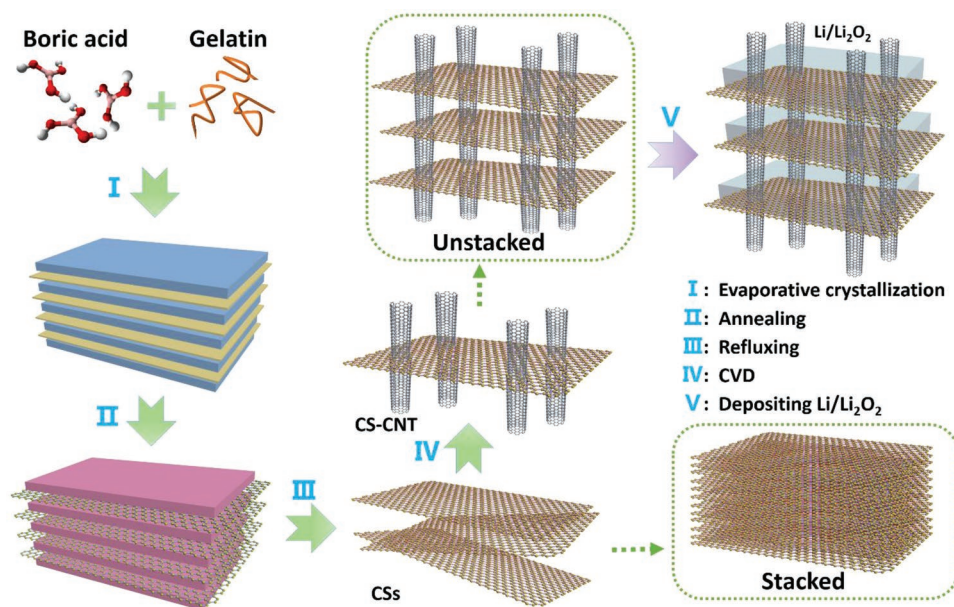
Dr. C. Zhao, Dr. Z. Song, Y. Sun, R. Li, Prof. X. Sun
Department of Mechanical and Materials Engineering
University of Western Ontario
London, ON N6A 5B9, Canada
E-mail: xsun9@uwo.ca

Dr. C. Zhao, Z. Wang, X. Tan, H. Huang, S. Cui, Q. Wei, W. Guo,
Prof. C. Yu, Prof. J. Qiu
State Key Lab of Fine Chemicals
Liaoning Key Lab for Energy Materials and Chemical Engineering
School of Chemical Engineering
Dalian University of Technology
Dalian 116024, China
E-mail: chang.yu@dlut.edu.cn; jqiu@dlut.edu.cn,
qiujs@mail.buct.edu.cn

Prof. J. Qiu
College of Chemical Engineering
Beijing University of Chemical Technology
Beijing 100029, China

 The ORCID identification number(s) for the author(s) of this article can be found under <https://doi.org/10.1002/smt.201800546>.

DOI: 10.1002/smt.201800546



Scheme 1. Schematic process for synthesis of CS-CNT and its behavior as the host material for Li metal anode and Li–O₂ battery air electrode.

the 3D conductive matrix can effectively mitigate the volume change of Li metal, especially with a large capacity.^[10] Recent efforts in the construction of 3D conductive matrix have proven efficacious for mitigating the growth of dendritic Li and improving the electrochemical performance.^[11]

Carbon materials feature light density, high conductivity, chemical stability, and good lithium affinity, which are considered as promising host materials for Li metal deposition.^[10b,12] So far, various carbon nanomaterials with different dimensions have been investigated and demonstrate enhanced electrochemical performance in LMBS, such as 2D graphene, 1D carbon nanofibers and carbon nanotubes (CNTs), and 0D nanospheres.^[13] However, the easy aggregation properties of carbon materials caused by the high surface energy and strong π - π interaction force can trigger the loss of specific surface area and pores, which limit the efficacy of carbon nanomaterials.^[3b,14] Therefore, configuring the unstacked carbon nanomaterials with sufficient surface area and porosity for holding the Li metal is considered to be an effective method to address the dendritic Li growth and volume change problems.

Herein, a green and scalable strategy was developed to convert the biomass to large-size N-doped carbon nanosheets (CSs). Subsequently, a unique 3D microstructure was constructed to address the aggregation problem of CSs, in which N-doped CNT forest was planted on the surface of CSs (CS-CNT). Benefiting from the unstacked nature, the as-prepared CS-CNT architecture can keep the porous structure under a harsh condition. As the host material for Li metal anode, doped N species are able to improve the wettability for Li metal and enable the uniform nucleation of metallic Li. The unstacked structure has the ability to provide large surface area and space for Li plating, rendering low local current density and dendrite-free Li deposition. More importantly, the cells delivered high and stable Coulombic efficiency of average 98.8% for over 2000 h, superior to pure CSs electrode and Cu foil electrode. The Li metal

symmetric cells assembled with CS-CNT@Li anodes exhibited significantly enhanced cycling life up to 1500 h as well as lower hysteresis. Furthermore, coupling CS-CNT@Li with a LiFePO₄ cathode for a full cell, it delivered enhanced specific capacity. Meanwhile, as the host material for Li–O₂ battery air electrode, the as-prepared CS-CNT also exhibited high specific capacity of more than 5000 mAh g⁻¹.

2. Results and Discussion

The typical synthetic process of CS-CNT is schematically illustrated in **Scheme 1**. Briefly, the CS-CNT was synthesized by a combined strategy involving a green template method to prepare large-size N-doped CSs from biomass and then a chemical vapor deposition (CVD) method to grow N-doped CNTs on CSs surface. First, a mixed solution of boric acid and gelatin was prepared. When the boric acid was being crystallized induced by continuous evaporation, a gelatin layer was formed in-between the layered structure of boric acid crystals. After annealing, the gelatin layers were converted to N-doped CSs, and the boric acid was decomposed to boron oxide. Through a refluxing process, the boron oxide was dissolved into water, yielding N-doped CSs.^[15] Here, the dissolved boron oxide can be recycled after drying. Finally, a typical CVD process was adopted to grow N-doped CNTs on the surface of N-doped CSs by using acetonitrile as the carbon and nitrogen sources, forming an unstacked microstructure of CS-CNT which is supposed to be a promising host matrix for Li metal anode and air electrode for Li–O₂ battery.

As shown in **Figure 1a**, the as-prepared CSs feature a typical sheet-shaped structure with a large size and thin thickness, highlighting the novel synthetic strategy of using boric acid as the template. However, 2D CSs usually tend to stack together and form a bulk due to the uniform sheet-shaped structure,

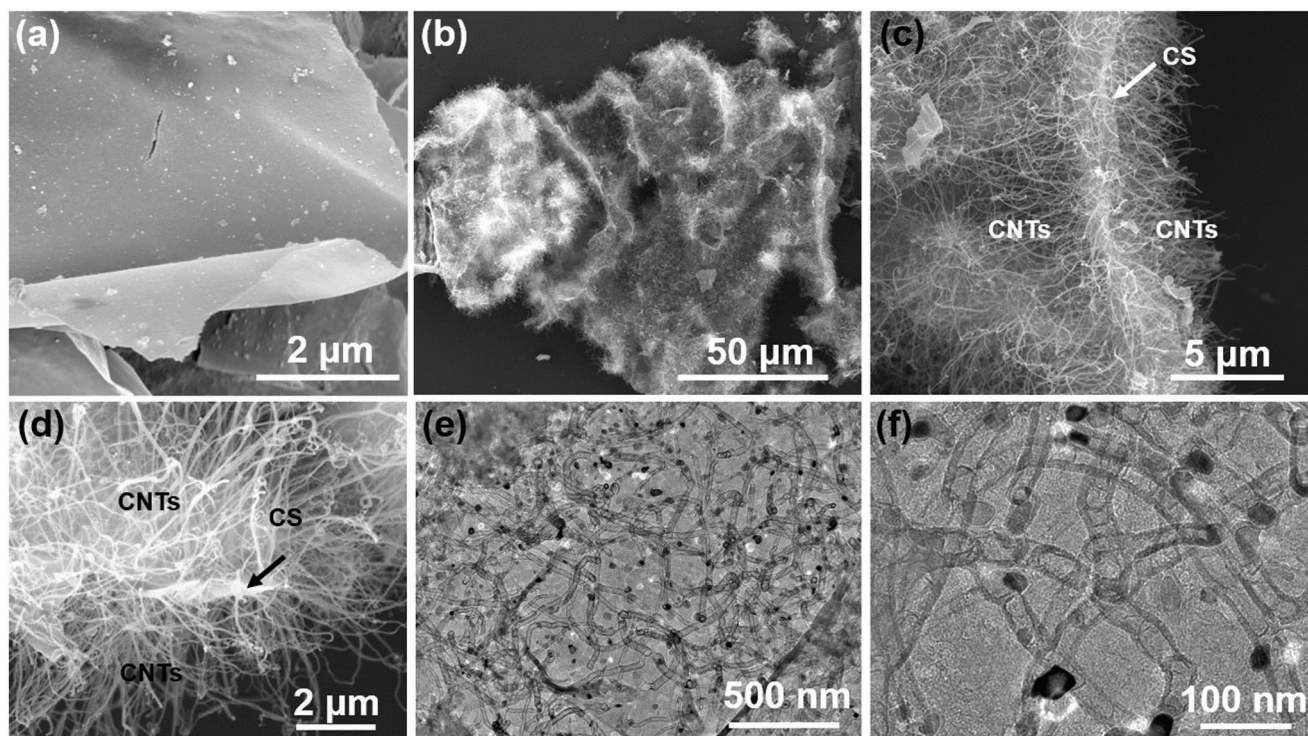


Figure 1. a) SEM image of the as-prepared CSs. b–d) SEM and e, f) TEM images of the as-prepared CS-CNT.

high surface energy, and strong π - π interaction force.^[14] As shown in Figure S1 in the Supporting Information, the CSs obtained by vacuum filtration display seriously stacked structure with few available pores, losing the advantages of 2D nanosheets such as high surface area and large pore volume. To overcome this problem, a modified structure was designed and developed. As shown in Figure 1b–d, it can be noted that CNT forest is planted on the surface of CSs. The CNTs serve as supports in preventing the aggregation of CSs.^[14] This can be evidenced by the SEM images of the CS-CNT microstructure after vacuum filtration (Figures S2 and S3, Supporting Information). It is worth noting that the CS-CNT microstructures effectively maintain the porous structure and overcome the stacked nature like CSs. The unstacked nature of CS-CNT can also be confirmed by nitrogen adsorption technique. As shown in Figure S4 in the Supporting Information, the as-made CS-CNT ($272 \text{ m}^2 \text{ g}^{-1}$) shows a larger N_2 adsorptive amount than CSs ($123 \text{ m}^2 \text{ g}^{-1}$), indicating a higher specific surface area. The pore volume of CS-CNT is $0.67 \text{ cm}^3 \text{ g}^{-1}$, almost twice as much as the CSs ($0.34 \text{ cm}^3 \text{ g}^{-1}$). Moreover, the pore-size distribution profiles indicate that the CS-CNT features a larger pore size than CSs. As the host materials for Li metal anode and air electrode for Li- O_2 battery, the unstacked CS-CNT microstructure will be in favor of the storage of Li metal and discharge products. Besides, the unstacked feature of CS-CNT can also retain the high surface area, avoiding the loss like CSs. The detailed structure of CS-CNT was further investigated by transmission electron microscopy (TEM) and the results are shown in Figure 1e, f. It can be noted that CNTs with a diameter of $\approx 40 \text{ nm}$ are uniformly planted on the surface of CSs. The unique bamboo structure of CNTs indicates their N-doped feature.

The composition and surface chemical states of the as-prepared CS-CNT were further examined by X-ray diffraction (XRD) technique, Raman spectroscopy, and X-ray photoelectron spectroscopy (XPS). As shown in Figure 2a, the XRD pattern of CSs shows a wide characteristic peak of graphite (002) at 26° , indicating an amorphous carbon nature of CSs.^[14b] By contrast, the characteristic peak at 26° of CS-CNT is stronger than that of CSs, which is due to the formation of CNTs with graphitized structure.^[16] Meanwhile, some peaks corresponding to Ni metal catalyst are present. The Raman spectra of CSs and CS-CNT reveal two remarkable peaks, corresponding to the D-band (1340 cm^{-1}) and G-band (1595 cm^{-1}) of carbon, respectively (Figure 2b). The I_D/I_G value of CS-CNT is 0.87, which is lower than that of CSs (1.05), indicating higher graphitization of CS-CNT than CSs.^[17] This is due to the formation of CNTs on the surface of CSs in the microstructure of CS-CNT. The surface chemistry of CS-CNT was further investigated by XPS. Figure S5 in the Supporting Information reveals that CS-CNT is mainly composed of C, N, O, and Ni elements. The C 1s XPS spectra of CS-CNT can be resolved into three components of C-C/C=C (284.6 eV), C-O/C-N (285.5 eV), and O=C-O (289.0 eV), respectively (Figure 2c).^[14b] The N 1s XPS spectra of CS-CNT reveal that the N species in CS-CNT are pyridinic and quaternary type of N atoms which exist in CSs and CNTs (Figure 2d).^[14a,17] The N element in CSs and CNTs are derived from the sources of gelatin and acetonitrile, respectively. The total N content in CS-CNT was determined to be about 10.0 at%. As reported in literature, the N species doped in carbon can improve the wettability for Li metal and benefit for the uniform nucleation and deposition of Li metal. The existence and distribution of N element can be detected by

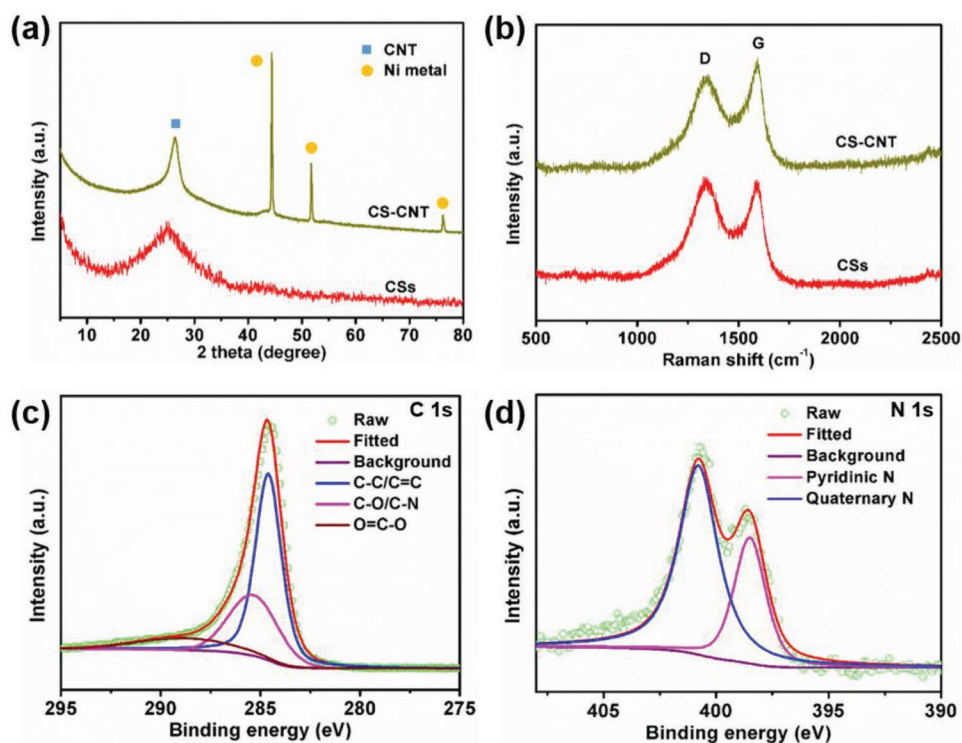


Figure 2. a) XRD patterns and b) Raman spectra of the as-prepared CSs and CS-CNT. c) C 1s and d) N 1s XPS spectra of the as-prepared CS-CNT.

the energy-dispersive X-ray spectroscopy (EDX) elemental mapping. As shown in Figure S6 in the Supporting Information, N element shows a similar distribution to C element in CS-CNT matrix, indicating the homogeneous distribution of N atoms.

Benefitting from these integrated characteristics of CS-CNT, the as-prepared CS-CNT as a host material may exhibit the unique superiority in regulating Li deposition. As shown in Figure S7 in the Supporting Information, the thickness of CS-CNT electrode is 36 μm , and the CS-CNT still keeps the unstacked structure. As shown in Figure 3a, after plating 0.3 mAh cm^{-2} of Li metal at a current density of 0.5 mA cm^{-2} , the metallic Li begins to nucleate and grows on the surface of CS-CNT. With the increase of Li deposition to 1 mAh cm^{-2} , the metallic Li can uniformly grow on the surface of CS-CNT. Notably, the surface of CS-CNT is not completely covered

by metallic Li even though a large amount of Li metal (about 5 μm) was deposited (Figure S8a, Supporting Information). By contrast, the controlled CSs electrode is fully covered by Li metal under the same amount of plated Li, which is due to the stacked structure of CSs that enables the nucleation easily on the surface of electrode rather than inside (Figure S8b, Supporting Information). This highlights the unstacked feature of this microstructure for rendering uniform Li deposition and accommodating the large volume change.^[13b] The magnified SEM image in Figure 3b shows that the deposited Li metal has a good contact with CS-CNT matrix and features the dendrite-free behavior, suggesting the effect of the doped N species and the high specific surface area of CS-CNT in regulating Li deposition.^[18] The existence of Li metal in the microstructure of CS-CNT can be confirmed by the morphology change of

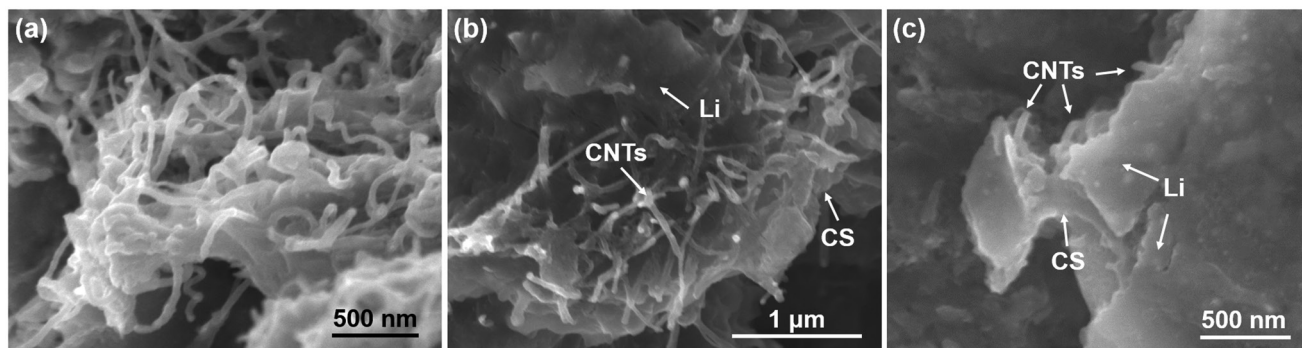


Figure 3. SEM images of the CS-CNT microstructure after discharging to a) 0.3 mAh cm^{-2} , b) 1 mAh cm^{-2} , and c) 3 mAh cm^{-2} .

CS-CNT electrode with 1 mAh cm^{-2} of Li metal. As shown in Figure S9 in the Supporting Information, the Li metal gradually melts under the electron beam and CNTs are gradually exposed. When the capacity of plated Li metal is increased to 3 mAh cm^{-2} , the CNTs on the surface of CSs have been totally covered by Li metal presented in a sandwich structure (Figure 3c). However, the CSs electrode shows a denser structure, which is completely coated by the Li metal (Figure S10, Supporting Information). In sharp contrast, the control sample of Cu foil electrode shows obvious Li dendrites when discharging to the areal capacity of 3 mAh cm^{-2} (Figure S11, Supporting Information). Based on the discussions above, the designed CS-CNT microstructure with the merits of doped N species and unstacked structure offers sufficient nucleation sites, large surface area, and space for smooth and uniform

Li deposition in this microstructure without dendritic Li. The composition of SEI layer in the CS-CNT electrode was examined by XPS. It is found that the SEI layer consists of inorganic and organic components such as alkyl lithium and lithium fluoride (Figure S12, Supporting Information).

The electrochemical performances of CS-CNT as the Li metal host were investigated via galvanostatic discharge/charge measurements. First, Coulombic efficiency was evaluated by examining the ratio of Li stripped capacity to Li plated capacity in each cycle. Coulombic efficiency of Li metal battery is a key parameter used for evaluating the sustainability of a Li metal anode and the Li metal deposition behavior.^[19] This is usually studied based on a half cell with the host material as the work electrode and Li metal as the counter electrode. As shown in Figure 4a, with a limited capacity of 1 mAh cm^{-2} and a current

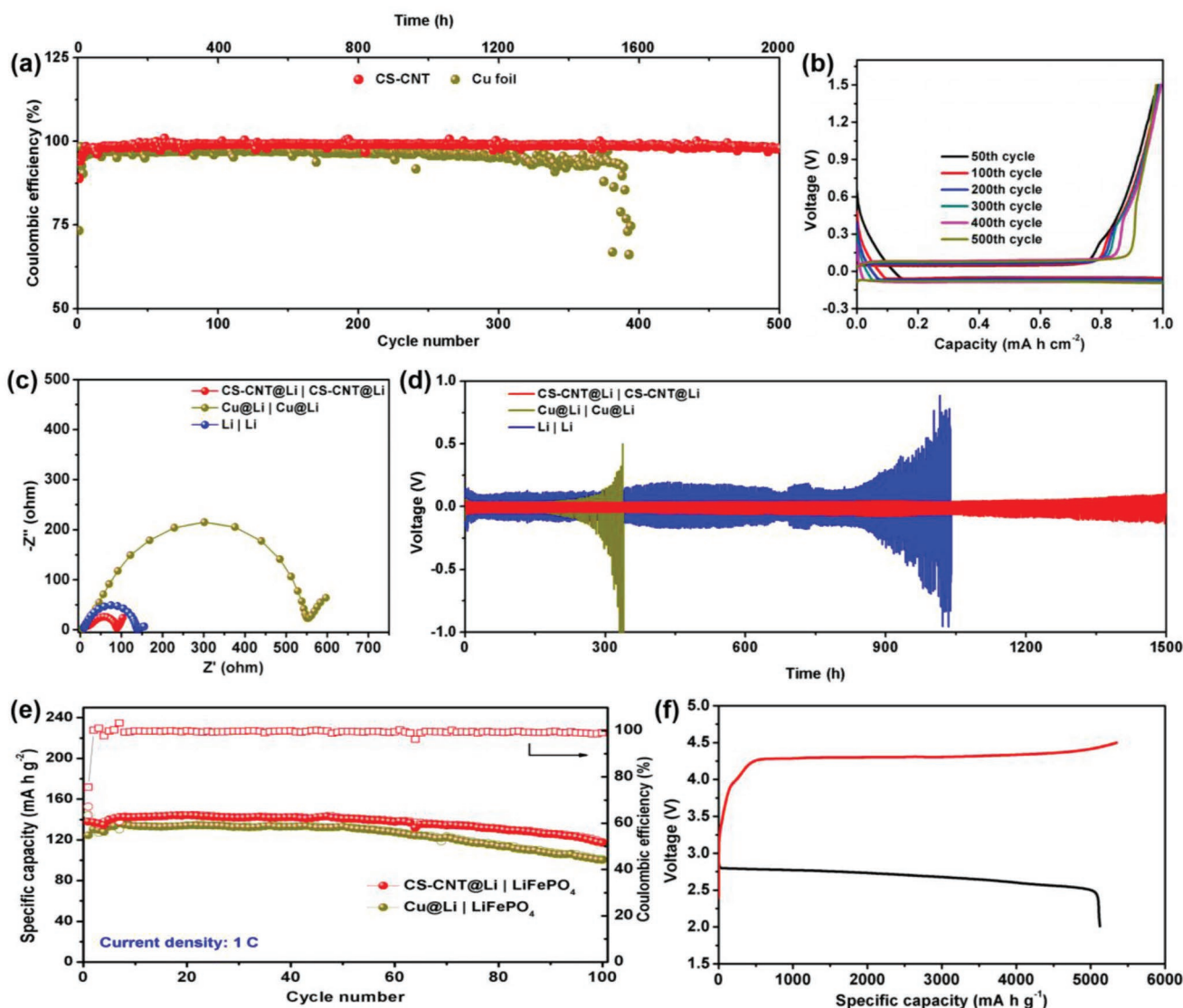


Figure 4. a) Coulombic efficiency of CS-CNT and Cu foil electrodes with a limited capacity of 1 mAh cm^{-2} at a current density of 0.5 mA cm^{-2} . b) The corresponding discharge/charge profiles of the CS-CNT electrode. c) Nyquist plots of the various symmetric cells. d) Cycle performances of various symmetric cells with a limited capacity of 1 mAh cm^{-2} at 0.5 mA cm^{-2} . e) Cycle performances of LiFePO₄ full cells with CS-CNT@Li and Cu@Li anodes at 1 C. f) Discharge/charge profiles of CS-CNT as the air electrode for Li-O₂ battery.

density of 0.5 mA cm^{-2} , the CS-CNT electrode exhibits an initial Coulombic efficiency of as high as 88.8% which is higher than 73.3% of pure Cu foil and 74.8% of CSs electrode (Figure S12, Supporting Information). Notably, CS-CNT electrode can keep high and stable Coulombic efficiency of average 98.8% for over 2000 h. In sharp contrast, Cu foil shows an average Coulombic efficiency of 95.6%, and the stable Coulombic efficiency is only able to be sustained for 1200 h, and the CSs electrode also shows a low Coulombic efficiency (Figure S13, Supporting Information). The high and stable Coulombic efficiency of CS-CNT electrode reveals the good reversibility of Li metal, superior Li deposition behavior and stable SEI layer. The low Coulombic efficiency of Cu foil electrode is due to more irreversible reactions between Li metal and electrolyte associated with the undesirable Li metal deposition and the formation of Li dendrites.^[20] The fluctuating Coulombic efficiency of Cu foil is related to the fracture of Li dendrites and the occasional reconnection of the fractured pieces.^[20] Although the electrode with high surface area will result in an increased initial SEI layer formation, but the electrode with merits of suppressing Li dendrites and accommodating the large volume change can effectively decrease the fracture of SEI layer and side reactions. Thus, the as-made CS-CNT electrode exhibited a higher Coulombic efficiency than the planar Cu electrode. The low Coulombic efficiency of CSs electrode is due to the low available surface area and little pore volume caused by the easy aggregation nature of CSs. The corresponding discharge/charge profiles of the CS-CNT also reveal the stable discharge/charge process and high Coulombic efficiency (Figure 4b). The electrochemical performances of symmetric cells were evaluated after preplating Li metal. As shown in Figure 4c, the CS-CNT@Li electrode shows the lowest resistance of charge transfer than that of Cu foil@Li and pure Li foil electrodes, indicating better existence of Li metal in CS-CNT@Li. The cycling stability of various symmetric cells was tested with a limited capacity of 1 mAh cm^{-2} at 0.5 mA cm^{-2} . Interestingly, symmetric cell with CS-CNT@Li electrodes exhibits the lowest hysteresis as well as significantly enhanced cycle life for over 1500 h (Figure 4d). On the contrary, Cu@Li anode and CSs@Li anode show short cycle life (Figure S14, Supporting Information), and Li foil delivers a higher hysteresis.

In order to explore the practicability and advantages of CS-CNT@Li anode, the full cell was built by coupling Li metal anode with LiFePO_4 cathode and tested at 1 C. As shown in Figure 4e, the full cell with CS-CNT@Li anode exhibits a higher specific capacity than that with Cu foil@Li anode and 84.8% of capacity retention after 100 cycles. Besides, according to the nature of the formation of the insoluble discharge products with low electronic conductivity in the air electrode of Li-O_2 batteries, the host materials with developed pore structure and large pore volume are desired to allow for the storage of a large amount of discharge products and achieve the high energy density. Based on the porous and untacked structure, the as-prepared CS-CNT was employed as the air electrode for Li-O_2 battery. As shown in Figure 4f, the CS-CNT delivers a high specific capacity of more than 5000 mAh g^{-1} , indicating the wide practicability. Meanwhile, the Ni particles in CNTs can play the role of catalyst to accelerate the discharge and charge processes.^[21]

3. Conclusions

In summary, we have successfully designed and constructed an unstacked microstructure of N-doped CNT forest planted on the surface of N-doped CSs. The unique architecture of CS-CNT possesses the porous structure and high specific surface area. Benefitting from these merits, the CS-CNT composite is used as the host materials for Li metal anode and exhibits excellent performance, evidenced by the high and stable Coulombic efficiency of average 98.8% and significantly enhanced cycle life for over 1500 h as well as lowered hysteresis. The present study sheds light on the design unstacked porous carbon materials and offers an opportunity to develop high efficiency Li metal anode.

Supporting Information

Supporting Information is available from the Wiley Online Library or from the author.

Acknowledgements

C.Z. and Z.W. contributed equally to this work. This work was partly supported by the National Natural Science Foundation of China (NSFC, Grant Nos. 21522601 and U1508201), the National Key Research and Development Program of China (Grant No. 2016YFB0101201), the (NSERC), the Canada Research Chair Program (CRC), the Canada Foundation for Innovation (CFI), and the Western University.

Conflict of Interest

The authors declare no conflict of interest.

Keywords

carbon nanosheets, carbon nanotubes, Li-O_2 batteries, lithium metal anodes, unstacked microstructures

Received: December 25, 2018

Revised: January 21, 2019

Published online:

- [1] a) M. Armand, J. M. Tarascon, *Nature* **2008**, *451*, 652; b) C. Zhao, C. Yu, M. Zhang, Q. Sun, S. Li, M. Norouzi Banis, X. Han, Q. Dong, J. Yang, G. Wang, X. Sun, J. Qiu, *Nano Energy* **2017**, *41*, 66; c) C. Zhao, C. Yu, B. Qiu, S. Zhou, M. Zhang, H. Huang, B. Wang, J. Zhao, X. Sun, J. Qiu, *Adv. Mater.* **2018**, *30*, 1702486; d) C. Zhao, C. Yu, M. Zhang, H. Huang, S. Li, X. Han, Z. Liu, J. Yang, W. Xiao, J. Liang, X. Sun, J. Qiu, *Adv. Energy Mater.* **2017**, *7*, 1602880.
- [2] a) P. G. Bruce, S. A. Freunberger, L. J. Hardwick, J.-M. Tarascon, *Nat. Mater.* **2012**, *11*, 19; b) Y. Yang, G. Zheng, Y. Cui, *Chem. Soc. Rev.* **2013**, *42*, 3018; c) A. C. Luntz, B. D. McCloskey, *Chem. Rev.* **2014**, *114*, 11721; d) A. Manthiram, Y. Fu, Y.-S. Su, *Acc. Chem. Res.* **2013**, *46*, 1125.
- [3] a) D. Lin, Y. Liu, Y. Cui, *Nat. Nanotechnol.* **2017**, *12*, 194; b) C. Zhao, C. Yu, M. N. Banis, Q. Sun, M. Zhang, X. Li, Y. Liu, Y. Zhao, H. Huang, S. Li, X. Han, B. Xiao, Z. Song, R. Li, J. Qiu, X. Sun,

- Nano Energy* **2017**, *34*, 399; c) J. Lu, L. Li, J.-B. Park, Y.-K. Sun, F. Wu, K. Amine, *Chem. Rev.* **2014**, *114*, 5611; d) S. Li, M. Jiang, Y. Xie, H. Xu, J. Jia, J. Li, *Adv. Mater.* **2018**, *30*, 1706375; e) Y. Kim, D. Koo, S. Ha, S. C. Jung, T. Yim, H. Kim, S. K. Oh, D.-M. Kim, A. Choi, Y. Kang, K. H. Ryu, M. Jang, Y.-K. Han, S. M. Oh, K. T. Lee, *ACS Nano* **2018**, *12*, 4419.
- [4] a) E. Cha, M. D. Patel, J. Park, J. Hwang, V. Prasad, K. Cho, W. Choi, *Nat. Nanotechnol.* **2018**, *13*, 337; b) H. Duan, Y.-X. Yin, Y. Shi, P.-F. Wang, X.-D. Zhang, C.-P. Yang, J.-L. Shi, R. Wen, Y.-G. Guo, L.-J. Wan, *J. Am. Chem. Soc.* **2018**, *140*, 82; c) Q. Pang, X. Liang, A. Shyamsunder, L. F. Nazar, *Joule* **2017**, *1*, 871; d) J.-S. Kim, D. W. Kim, H. T. Jung, J. W. Choi, *Chem. Mater.* **2015**, *27*, 2780.
- [5] a) D. Lin, J. Zhao, J. Sun, H. Yao, Y. Liu, K. Yan, Y. Cui, *Proc. Natl. Acad. Sci. USA* **2017**, *114*, 4613; b) Z. Liang, D. Lin, J. Zhao, Z. Lu, Y. Liu, C. Liu, Y. Lu, H. Wang, K. Yan, X. Tao, Y. Cui, *Proc. Natl. Acad. Sci. USA* **2016**, *113*, 2862; c) Y. iu, D. Lin, Z. Liang, J. Zhao, K. Yan, Y. Cui, *Nat. Commun.* **2016**, *7*, 10992; d) D. Lin, Y. Liu, W. Chen, G. Zhou, K. Liu, B. Dunn, Y. Cui, *Nano Lett.* **2017**, *17*, 3731; e) A. Wang, X. Zhang, Y.-W. Yang, J. Huang, X. Liu, J. Luo, *Chemistry* **2018**, *4*, 2192.
- [6] a) Q. Li, S. Tan, L. Li, Y. Lu, Y. He, *Sci. Adv.* **2017**, *3*, e1701246; b) H. Zhang, X. Liao, Y. Guan, Y. Xiang, M. Li, W. Zhang, X. Zhu, H. Ming, L. Lu, J. Qiu, Y. Huang, G. Cao, Y. Yang, L. Mai, Y. Zhao, H. Zhang, *Nat. Commun.* **2018**, *9*, 3729; c) D. Lin, Y. Liu, A. Pei, Y. Cui, *Nano Res.* **2017**, *10*, 4003; d) Y. Zhao, Q. Sun, X. Li, C. Wang, Y. Sun, K. R. Adair, R. Li, X. Sun, *Nano Energy* **2018**, *43*, 368; e) Y. Sun, G. Zheng, Z. W. Seh, N. Liu, S. Wang, J. Sun, H. R. Lee, Y. Cui, *Chemistry* **2016**, *1*, 287; f) A. C. Kozen, C.-F. Lin, A. J. Pearse, M. A. Schroeder, X. Han, L. Hu, S.-B. Lee, G. W. Rubloff, M. Noked, *ACS Nano* **2015**, *9*, 5884.
- [7] a) C. Yang, L. Zhang, B. Liu, S. Xu, T. Hamann, D. McOwen, J. Dai, W. Luo, Y. Gong, E. D. Wachsman, L. Hu, *Proc. Natl. Acad. Sci. USA* **2018**, *115*, 3770; b) N.-W. Li, Y. Shi, Y.-X. Yin, X.-X. Zeng, J.-Y. Li, C.-J. Li, L.-J. Wan, R. Wen, Y.-G. Guo, *Angew. Chem., Int. Ed.* **2018**, *57*, 1505.
- [8] a) J. Zheng, M. H. Engelhard, D. Mei, S. Jiao, B. J. Polzin, J.-G. Zhang, W. Xu, *Nat. Energy* **2017**, *2*, 17012; b) M. D. Tikekar, S. Choudhury, Z. Tu, L. A. Archer, *Nat. Energy* **2016**, *1*, 16114; c) F. Ding, W. Xu, G. L. Graff, J. Zhang, M. L. Sushko, X. Chen, Y. Shao, M. H. Engelhard, Z. Nie, J. Xiao, X. Liu, P. V. Sushko, J. Liu, J.-G. Zhang, *J. Am. Chem. Soc.* **2013**, *135*, 4450; d) E. Kazayak, K. N. Wood, N. P. Dasgupta, *Chem. Mater.* **2015**, *27*, 6457; e) X. Zhang, Q. Zhang, X.-G. Wang, C. Wang, Y.-N. Chen, Z. Xie, Z. Zhou, *Angew. Chem., Int. Ed.* **2018**, *57*, 12814.
- [9] a) X. Ji, D.-Y. Liu, D. G. Prendiville, Y. Zhang, X. Liu, G. D. Stucky, *Nano Today* **2012**, *7*, 10; b) X.-B. Cheng, H.-J. Peng, J.-Q. Huang, R. Zhang, C.-Z. Zhao, Q. Zhang, *ACS Nano* **2015**, *9*, 6373.
- [10] a) C. Zhao, C. Yu, S. Li, W. Guo, Y. Zhao, Q. Dong, X. Lin, Z. Song, X. Tan, C. Wang, M. Zheng, X. Sun, J. Qiu, *Small* **2018**, *14*, 1803310; b) D. Lin, Y. Liu, Z. Liang, H.-W. Lee, J. Sun, H. Wang, K. Yan, J. Xie, Y. Cui, *Nat. Nanotechnol.* **2016**, *11*, 626; c) N. Li, W. Wei, K. Xie, J. Tan, L. Zhang, X. Luo, K. Yuan, Q. Song, H. Li, C. Shen, E. M. Ryan, L. Liu, B. Wei, *Nano Lett.* **2018**, *18*, 2067; d) L. Fan, H. L. Zhuang, W. Zhang, Y. Fu, Z. Liao, Y. Lu, *Adv. Energy Mater.* **2018**, *8*, 1703360.
- [11] a) R. Mukherjee, A. V. Thomas, D. Datta, E. Singh, J. Li, O. Eksik, V. B. Shenoy, N. Koratkar, *Nat. Commun.* **2014**, *5*, 3710; b) C. Jin, O. Sheng, J. Luo, H. Yuan, C. Fang, W. Zhang, H. Huang, Y. Gan, Y. Xia, C. Liang, J. Zhang, X. Tao, *Nano Energy* **2017**, *37*, 177; c) Q. Li, S. Zhu, Y. Lu, *Adv. Funct. Mater.* **2017**, *27*, 1606422; d) S.-S. Chi, Y. Liu, W.-L. Song, L.-Z. Fan, Q. Zhang, *Adv. Funct. Mater.* **2017**, *27*, 1700348; e) H. Zhao, D. Lei, Y.-B. He, Y. Yuan, Q. Yun, B. Ni, W. Lv, B. Li, Q.-H. Yang, F. Kang, J. Lu, *Adv. Energy Mater.* **2018**, *8*, 1800266.
- [12] a) A. Zhang, X. Fang, C. Shen, Y. Liu, C. Zhou, *Nano Res.* **2016**, *9*, 3428; b) S. Matsuda, Y. Kubo, K. Uosaki, S. Nakanishi, *Carbon* **2017**, *119*, 119; c) H. Ye, S. Xin, Y.-X. Yin, Y.-G. Guo, *Adv. Energy Mater.* **2017**, *7*, 1700530.
- [13] a) G. Zheng, S. W. Lee, Z. Liang, H.-W. Lee, K. Yan, H. Yao, H. Wang, W. Li, S. Chu, Y. Cui, *Nat. Nanotechnol.* **2014**, *9*, 618; b) S. Liu, A. Wang, Q. Li, J. Wu, K. Chiou, J. Huang, J. Luo, *Joule* **2018**, *2*, 184; c) C. Yang, Y. Yao, S. He, H. Xie, E. Hitz, L. Hu, *Adv. Mater.* **2017**, *29*, 1702714; d) Q. Song, H. Yan, K. Liu, K. Xie, W. Li, W. Gai, G. Chen, H. Li, C. Shen, Q. Fu, S. Zhang, L. Zhang, B. Wei, *Adv. Energy Mater.* **2018**, *8*, 1800564; e) A.-R. O. Raji, R. Villegas Salvatierra, N. D. Kim, X. Fan, Y. Li, G. A. L. Silva, J. Sha, J. M. Tour, *ACS Nano* **2017**, *11*, 6362.
- [14] a) C. Zhao, C. Yu, M. Zhang, J. Yang, S. Liu, M. Li, X. Han, Y. Dong, J. Qiu, *J. Mater. Chem. A* **2015**, *3*, 21842; b) C. Yu, C. Zhao, S. Liu, X. Fan, J. Yang, M. Zhang, J. Qiu, *Chem. Commun.* **2015**, *51*, 13233.
- [15] Z. Ling, Z. Wang, M. Zhang, C. Yu, G. Wang, Y. Dong, S. Liu, Y. Wang, J. Qiu, *Adv. Funct. Mater.* **2016**, *26*, 111.
- [16] M. Zhang, C. Yu, C. Zhao, X. Song, X. Han, S. Liu, C. Hao, J. Qiu, *Energy Storage Mater.* **2016**, *5*, 223.
- [17] C. Zhao, C. Yu, S. Liu, J. Yang, X. Fan, H. Huang, J. Qiu, *Adv. Funct. Mater.* **2015**, *25*, 6913.
- [18] R. Zhang, X.-R. Chen, X. Chen, X.-B. Cheng, X.-Q. Zhang, C. Yan, Q. Zhang, *Angew. Chem., Int. Ed.* **2017**, *56*, 7764.
- [19] R. Zhang, X.-B. Cheng, C.-Z. Zhao, H.-J. Peng, J.-L. Shi, J.-Q. Huang, J. Wang, F. Wei, Q. Zhang, *Adv. Mater.* **2016**, *28*, 2155.
- [20] R. Zhang, N.-W. Li, X.-B. Cheng, Y.-X. Yin, Q. Zhang, Y.-G. Guo, *Adv. Sci.* **2017**, *4*, 1600445.
- [21] a) Y. Chen, Q. Zhang, Z. Zhang, X. Zhou, Y. Zhong, M. Yang, Z. Xie, J. Wei, Z. Zhou, *J. Mater. Chem. A* **2015**, *3*, 17874; b) Z. Zhang, L. Su, M. Yang, M. Hu, J. Bao, J. Wei, Z. Zhou, *Chem. Commun.* **2014**, *50*, 776.